European Journal of Pharmacology 874 (2020) 173003

Contents lists available at ScienceDirect

European Journal of Pharmacology

journal homepage: www.elsevier.com/locate/ejphar

Full length article

# Naringin inhibits autophagy mediated by PI3K-Akt-mTOR pathway to ameliorate endothelial cell dysfunction induced by high glucose/high fat stress

Kun Wang[a,b,1], Shengjia Peng[c,d,1], Shaofeng Xiong[a,b], Ailin Niu[a,b], Min Xia[a,b], Xiaowei Xiong[a,b], Guohua Zeng[a,b], Qiren Huang[a,b,*]

[a] Provincial Key Laboratory of Basic Pharmacology, Nanchang University, Nanchang, Jiangxi, 330006, PR China
[b] Department of Pharmacology, School of Pharmacy, Nanchang University, Nanchang, Jiangxi, 330006, PR China
[c] Jiangxi Medical College, Nanchang University, Nanchang, Jiangxi, 330006, PR China
[d] Nanchang Joint Programme, Queen Mary University of London, Nanchang, Jiangxi, 330006, PR China

ARTICLE INFO

*Keywords:*
Naringin
Endothelial cell
Dysfunction
Autophagy
Stress

ABSTRACT

As a flavonoid, naringin (Nar) has been shown to have multiple pharmacological effects including lowering blood cholesterol, reducing thrombus formation and improving microcirculation. However, effects of Nar on function and autophagy of vascular endothelial cells under high glucose and high fat (HG/HF) stress are largely unclear. This study was designed to investigate such effects of Nar in human umbilical vein endothelial cells (HUVECs) and to determine whether such effects are related to autophagy. Our present results show that 86 μM of Nar inhibits the autophagy levels and protects the cells against the dysfunction induced by HG/HF stress. Moreover, Nar increases the phosphorylation levels of phosphatidylinositol-3-kinase (PI3K), protein kinase B (Akt) and mammalian rapamycin target protein (mTOR). However, pretreatment with rapamycin (RAPA, 5 μM, autophagy inducer), LY294002(10 μM, PI3K inhibitor) and Akt inhibitor IV (0.5 μM, Akt inhibitor) partially abrogates the protective effects of Nar, suggesting that the protective effects of Nar are achieved by activating the PI3K-Akt-mTOR pathway to inhibit autophagy. In conclusion, Nar improves the function of HUVECs under HG/HF stress through activating the PI3K-Akt-mTOR pathway to inhibit autophagy. The findings offer an insight into HG/HF stress-induced autophagy and indicate that Nar might have potential to prevent and treat the diabetic angiopathy.

## 1. Introduction

High-sugar or high-fat diets often appear in our meals that provide us with considerable energy intake. However, growing evidence shows that excessive intake of high-sugar and high-fat foods readily results in hyperglycemia, hyperlipidemia, obesity, insulin resistance, atherosclerosis and diabetes, which are known as metabolic syndrome (Soisungwan et al., 2017; Karuna et al., 2011). Vascular endothelial cells are located between blood and vascular tissue and have diverse functions, including barrier, permeability, migration, proliferative repair and endocrine. However, they are easily damaged by various physical, chemical and biological factors. The damaged vascular endothelial cells disturb homeostasis between constriction and dilation substances, leading to the cardiovascular disease.

Autophagy is an important cellular catabolic process in which useless proteins and damaged organelles are isolated in a double membrane-bound structure called autophagosomes (Ramkumar et al., 2017). The autophagosomes are then delivered to lysosomes and vacuoles for degradation. The autophagic degradation of membrane lipids and proteins produces free fatty acids and amino acids that can be reused to maintain the cell survival (Xilouri et al., 2016). For example, the activation of autophagy in the articular chondrocytes from osteoarthritic rats alleviates inflammation (Xue et al., 2017). Chaperone-mediated autophagy has a protective effect on galactose/lipopolysaccharide-induced acute liver failure in rats (Li and Lu et al., 2017). While autophagy maintains cell homeostasis by clearing damaged organelles and proteins, it also causes non-apoptotic programmed cell death (autophagic cell death) due to excessive autophagy or sustained

* Corresponding author. Key Provincial Laboratory of Basic Pharmacology, Nanchang University, 461 Ba-Yi Street, Nanchang, Jiangxi, 330006, PR China.
*E-mail address:* qrhuang@ncu.edu.cn (Q. Huang).
[1] Equal contribution to this article.

https://doi.org/10.1016/j.ejphar.2020.173003
Received 24 November 2019; Received in revised form 3 February 2020; Accepted 7 February 2020
Available online 08 February 2020

activation. Studies have reported that the excessive activation of autophagy is involved in autophagic death in ischemic injury, while inhibition of excessive autophagy can reduce neuronal death associated with cerebral ischemia (Shi et al., 2012). Glutamate-mediated oxidative stress induces autophagy in mouse hippocampal HT22 cells, which subsequently leads to autophagic death of neurons (Yin et al., 2016). It is well known that PI3K-Akt-mTOR pathway is involved in the regulation of autophagy (Lamoureux and Zoubeidi, 2013). Generally, activation of PI3K-Akt-mTOR pathway by nutrients promotes cell growth and proliferation whereas inhibition of this pathway results in autophagy (Dey et al., 2017; Heras-Sandoval et al., 2014).

The role of flavonoids in the prevention and treatment of chronic non-communicable diseases such as cardiovascular diseases and diabetes has attracted much attention (Vazhappilly et al., 2019). Naringin (Nar, $C_{27}H_{32}O_{14}$, molecular weight: 580.54), a citrus flavonoid found in Chinese sweet pomelo, grape seeds and so on, has anti-oxidative, anti-inflammatory and anti-atherosclerotic bioactivities (Lavrador et al., 2018). These properties indicate that Nar could be a promising drug candidate (Lavrador et al., 2018). Recent studies have reported that Nar protects cardiomyocytes against anoxia/reoxygenation-induced apoptosis (Chen et al., 2015). Other investigations have shown Nar improves mitochondrial dysfunction and reduces the inflammation in sodium iodate-induced rat osteoarthritis model (Kulasekaran and Ganapasam, 2015; Xu et al., 2017). However, effects of Nar on function and autophagy of vascular endothelial cells under HG/HF stress are largely unclear. In this study, we sought to investigate the regulatory effects of Nar on autophagy levels mediated by PI3K-Akt-mTOR pathway.

## 2. Materials and methods

### 2.1. Antibodies and chemicals

Rabbit polyclonal antibody against LC3B (ab48394), rabbit monoclonal antibody against Beclin1 (ab207612) and p-eNOS (Ser1177, ab215717), mouse monoclonal antibody against p62 (ab56416) and eNOS (ab76198) were purchased from Abcam (Cambridge, UK). Rabbit polyclonal anti-PI3K (4257S), anti-p-PI3K (Tyr458, 17366S), anti-Akt (9272S), anti-p-Akt (Ser 473,9271S), anti-mTOR (2983S) and anti-p-mTOR (Ser 2448, 5536S) were purchased from Cell Signaling Technology, Inc. (Danvers, MA, USA). Mouse polyclonal anti-GAPDH (60004-1-Ig) was purchased from *Proteintech* Biotechnology, Inc. (Wuhan, CHN). Peroxidase-Conjugated Goat anti-rabbit (ZB-5301) and anti-mouse IgG (ZB-5305) were purchased from ZSGB Biotechnology, Inc. (Beijing, CHN). Rapamycin (RAPA, an autophagy inducer) and 3-methyladenine (3-MA, an autophagy inhibitor) were purchased from MedChemExpress Inc. (New Jersey, USA). LY294002 (PI3K inhibitor) and Akt Inhibitor IV(Akt inhibitor) were purchased from APExBIO, Inc. (Houston, Texas, USA). Nitric oxide (NO, A012-1-2) and Lactate dehydrogenase (LDH, A020-2-1) assay kit were purchased from Nanjing Jiancheng Biotechnology, Inc. (Nanjing, CHN). Human endothelin-1 (ET-1) ELISA kit (bs-0188R) was purchased from Jianglai Biological Technology Co, (Shanghai, CHN). BCA protein assay kit (P0010) and reactive oxygen species assay kit (S0033) were purchased from Beyotime Biotechnology, Inc. (Shanghai, CHN). Low-glucose DMEM containing 5.5 mM glucose was purchased from Solarbio (Beijing, CHN). Anhydrous glucose powder was purchased from Sigma-Aldrich (Saint Louis, US). All other chemicals are the highest grade and commercially available.

### 2.2. Cell culture

HUVECs were obtained from ATCC®CRL-1730™. Cells were cultured following the method as described routinely with a minor modification. Briefly, the cells were grown in Dulbecco's modified Eagle's medium (DMEM) supplemented with 10% fetal bovine serum (FBS), penicillin-streptomycin (Gibco Life Technologies, Carlsbad, CA, USA), and 1% endothelial cell growth supplement (ECGS) (ScienCell, SanDiego, California, USA), and incubated at 37 ˚C in a humidified incubator with 5% $CO_2$. The cells used in all experiments are the passage 6.

### 2.3. Preparation of high glucose and high fat solution

To prepare 11 mM, 22 mM, 33 mM, 44 mM and 55 mM of glucose, 0.05 g, 0.15 g, 0.25 g, 0.35 g and 0.45 g of anhydrous glucose powder were weighed and dissolved in 50 ml of low-glucose DMEM, respectively. The solutions were filtered by 0.22 μm microporous filter membrane in aseptic console and stored at 4 ˚C. To prepare different concentrations of high fat solutions, i.e., 0.125 mM, 0.25 mM, 0.5 mM, 1.0 mM and 2.0 mM, respectively, the stock solution of high fat was prepared. Briefly, 51.28 mg of palmitic acid (PA) was completely dissolved in 1.0 ml anhydrous ethanol by vortex. 10% of bovine serum albumin (BSA) solution was made and the PA and 10% BSA were mixed in the ratio of 1:19 (263 μl: 5 ml) and were fully dissolved at 55 ˚C water bath. The mixture was filtered with 0.45 μm microporous filter membrane in aseptic manner to prepare 10 mM PA stock solution which was stored at -20 ˚C. Upon used, the PA stock solution was diluted into the desired concentration.

### 2.4. Hematoxylin and eosin (H & E) staining

HUVECs were cultured in 6-well plates at $2 \times 10^5$ cells for 24 h. After different treatments, the cells were fixed for 20 min with 95% of ethyl alcohol. Subsequently, the cells were gently washed twice with phosphate-buffered saline (PBS). Then the cells were stained with hematoxylin for 3 min and eosin for 1 min in the dark at room temperature. Finally, the cells were visualized under an inverted microscope (Olympus, Japan).

### 2.5. Reactive oxygen species assay

The production of intracellular reactive oxygen species was monitored with a reactive oxygen species detection kit according to the manufacturer's instructions. Fluorescent probe 2, 7- dichlorodihydrofluorescein diacetate (DCFH-DA) is catalyzed by intracellular esterases and converted to DCFH which is further oxidized to the highly fluorescent dichlorofluorescin (DCF) in the presence of reactive oxygen species. Because fluorescence intensity of DCF is proportional to the level of reactive oxygen species, it is well expressed as the level of reactive oxygen species. Briefly, DCFH-DA was diluted with serum-free medium at 1:1000, and its final concentration was 10 μM. HUVECs were collected and suspended in diluted DCFH-DA, and then the cells were incubated for 20 min at 37 ˚C. Subsequently, the cells were washed twice with PBS to fully remove DCFH-DA that has not entered the cells. Finally, the relative levels of reactive oxygen species were assessed using the fluorescence intensity of DCF detecting by flow cytometer (Beckman Coulter, Inc., California,USA) and the DCF fluorescence intensity was quantified.

### 2.6. MTT assay

A modified MTT assay was used to evaluate cell viability. Cells were seeded into a 96-well plate at a density of $5 \times 10^3$ cells per well.When grown to 95% confluency, the cells were treated with various HG/HF concentration combinations including 11/0.125, 22/0.25, 33/0.5, 44/1.0 and 55/2.0 mM for 24 h. The cells were then treated with MTT (at a concentration of 5 mg/ml, Sigma-Aldrich) for 4 h in a humidified incubator with 5% $CO_2$ at 37 ˚C. Next, the supernatant was discarded. And then, DMSO was added to dissolve formazan. Finally, the optical density (OD) was measured at 490 nm using a microplate reader (BIO-RAD, USA). The viability of the non-treated cells (Control) was defined as 100%, and the viability of cells from all other groups was expressed

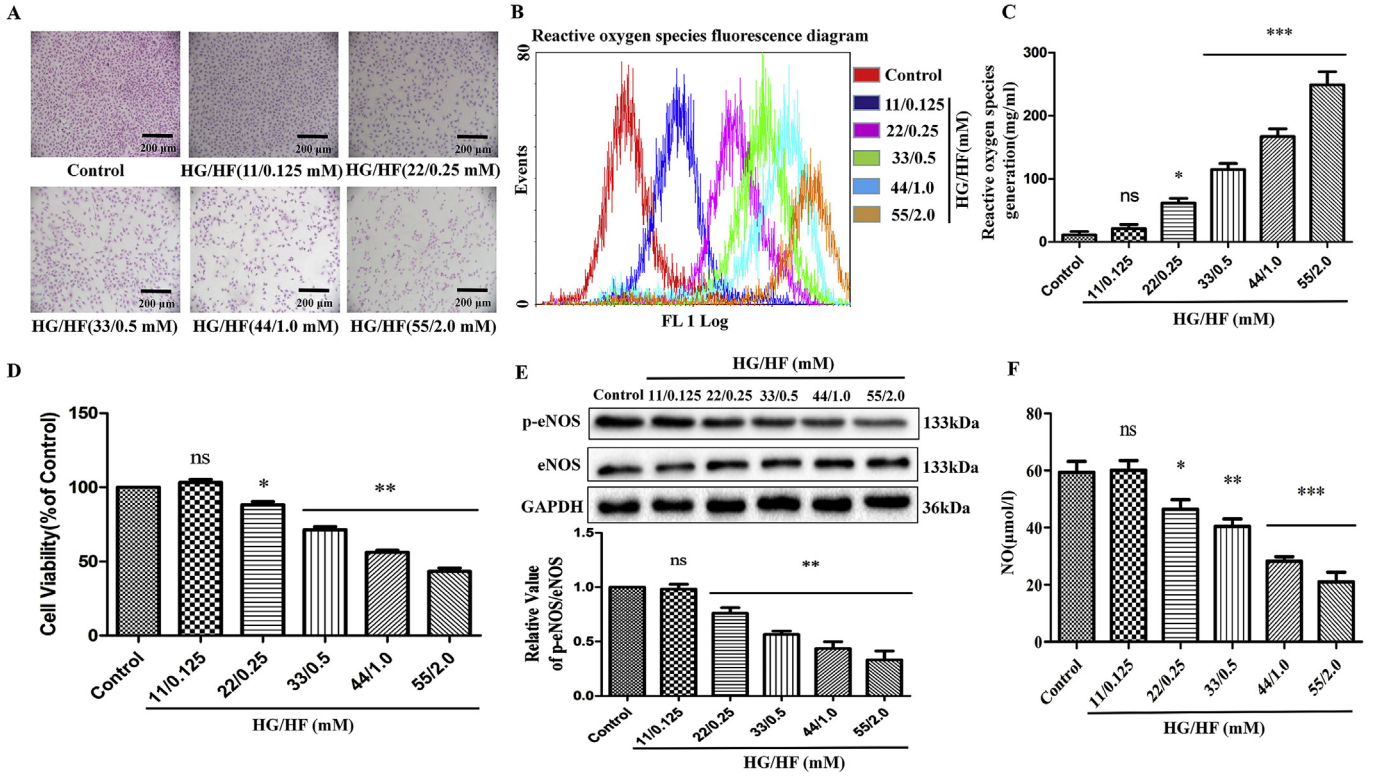


**Fig. 1.** HG/HF stress causes dysfunction of HUVECs in a concentration-dependent manner. 95% confluent HUVECs were respectively exposed to various glucose/palmitic acid (PA) concentration combinations including control (5.5/0 mM) and HG/HF (11/0.125, 22/0.25, 33/0.5, 44/1.0 and 55/2.0 mM) for 24 h. The cell morphology (A, H&E staining), reactive oxygen species generation (B and C, flow cytometry), cell viability (D), p-eNOS (E) and NO levels (F) were detected. GAPDH was considered as a loading control. Data are expressed as mean ± S.E.M. of 3 independent experiments. Student's t-test and ANOVA were performed. $*P < 0.05$, $**P < 0.01$, $***P < 0.001$, *vs.* Control group; ns: no significant difference. p-eNOS: phosphorylated endothelial NO synthase, HG/HF: high glucose/high fat, NO: nitric oxide. Scale bar in A: 200 μm.

as the percent (%) of the Control group.

### 2.7. Western blotting

Western blotting was performed according to the method described in our previous study with a minor modification (Zhang et al., 2015). Briefly, cells were washed twice with PBS, disrupted on ice for 30 min in NP-40 (50 mM Tris (pH 7.4), 1% NP-40, 150 mM NaCl and 40 mM NaF) or RIPA lysis buffer (Thermo Scientific, Shanghai, CHN) supplemented with the protease and phosphatase inhibitors (Pierce Chemical, Dallas, US) and cleared by centrifugation. Protein concentration was determined with a BCA protein quantification kit. A total of 50 μg of protein was loaded onto SDS-PAGE gels and then transferred onto polyvinylidene difluoride (PVDF) membranes (0.45 μm and 0.22 μm, Millipore, MA, USA). After being blocked for 2 h in 5% skim milk, the PVDF membranes were washed with Tris-buffered saline containing 0.1% Tween-20 (TBST) three times and incubated overnight at 4 °C with specific primary antibodies at 1:1000 dilution except for p62 (1:500) and GAPDH (1:4000) and secondary antibodies at a 1:4000 dilution. Then the results were detected by chemiluminescence with the ECL detection reagents (Amersham Biosciences, London, UK). GAPDH was used as a loading control. The expression levels of all proteins were expressed as the ratio of GAPDH.

### 2.8. Measurement of NO, ET-1 and LDH release

HUVECs were cultured in 6-well plates at $2\times 10^5$ cells per well. After treatment, the supernatant was respectively used to measure the levels of NO, ET-1 and LDH release with their commercially available assay kits. The levels of NO and LDH release were detected by colorimetric assay and the ET-1 levels were measured by ELISA. The levels of NO are commonly indicated with nitrite levels. The levels of nitrite were determined with an assay kit according to the kit instructions. Briefly, a standard curve was prepared using a gradient of nitrite concentrations. 100 μl of samples were added onto a 96-well microplate, and then Griess reagent I and II were in turn added and mixed well. Next, the mixture was incubated at 37 °C for 60 min. Finally, OD values were determined at 550 nm with a spectrophotometer (Bio-Rad Laboratories).

### 2.9. Autophagosome detection by MDC staining

HUVECs were cultured on a cover slip in a confocal dish. When grown to 95% confluency, the cells were respectively undergone varied treatments according to the experiment protocol. Then, the cells were gently rinsed three times with PBS. Next, the cells were sequentially incubated with a preheated mondansylcadaverin (MDC) working solution for 30 min, and with DAPI counter-staining solution for 30 min at 37 °C. Finally, the cells were visualized and photographed under Deltavision$^{TM}$Ultra (GE Healthcare, Sweden).

### 2.10. Cell healing assay

HUVECs were cultured in a 6-well plate at $2\times 10^5$ cells for 24 h. Upon grown to 95% confluency, the cells were scratched off with a sterile 200 μl pipette tip along the pre-drawn lines on the bottom of the plate. The cells were washed gently twice with PBS to remove the cells shed off from the plate bottom. The intact cells were treated with a complete DMEM containing HG/HF in presence or absence of various concentrations of Nar for 48 h at 37 °C, 5% $CO_2$. The cells were

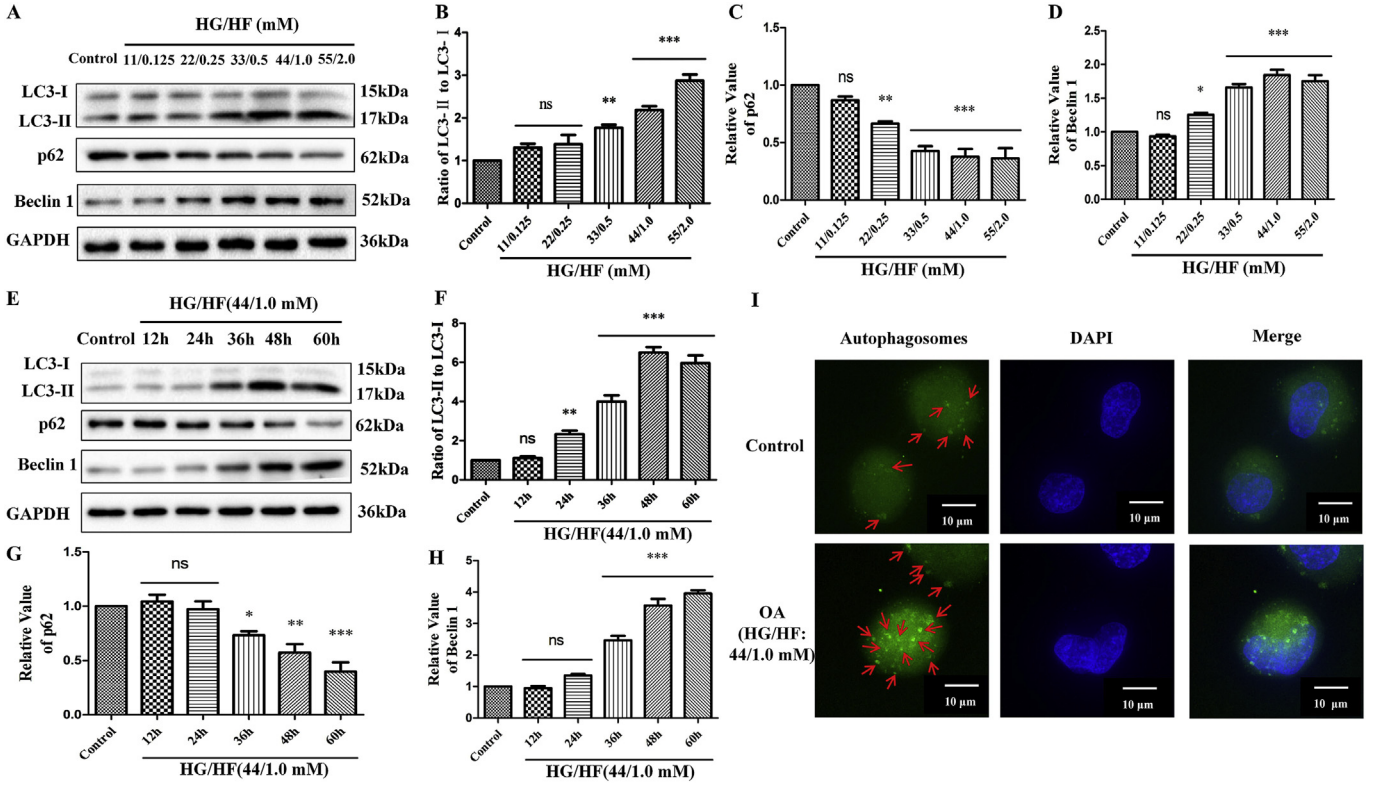


**Fig. 2.** HG/HF stress induces autophagy in a concentration-and time-dependent manner. 95% confluent HUVECs were respectively exposed to various glucose/palmitic acid (PA) concentration combinations including control (5.5/0 mM) and HG/HF (11/0.125, 22/0.25, 33/0.5, 44/1.0 and 55/2.0 mM) for 24 h. The expression levels of LC3-II/LC3-I (A, B), p62 (A, C) and Beclin 1 (A, D) were detected by western blotting. Besides, 95% confluent HUVECs were exposed to 44/1.0 mM of HG/HF for 0 h (Control), 12 h, 24 h, 36 h, 48 h and 60 h, respectively, and the expression levels of LC3-II/LC3-I (E, F), p62 (E, G) and Beclin 1 (E, H) were detected by western blotting. GAPDH was considered as a loading control. Meanwhile, another batch of 95% confluent HUVECs were exposed to 44/1.0 mM of HG/HF for 24 h (as the optimal autophagy, OA), and autophagosomes were visualized by MDC staining (I). Data are expressed as mean ± S.E.M. of 3 independent experiments. Student's t-test and ANOVA were performed. $^{*}P < 0.05$, $^{**}P < 0.01$, $^{***}P < 0.001$, *vs.* Control group; ns: no significant difference; scale bar for I is 10 μm. HG/HF: high glucose/high fat, OA: optimal autophagy condition (44/1.0 mM of HG/HF for 24 h).

visualized and photographed under an inverted microscope at 0 h, 24 h and 48 h after scratching and cell-healing rate (%) was calculated.

### 2.11. Cell migration assay

Cell migration assay was performed according to methods described by Wang et al. with a minor modification (Wang et al., 2018). Briefly, cells ($2\times10^4$) were seeded and cultured in the top chambers of a 24-well plates with an 8-mm transwell insert per well. 200 μl serum-free medium and 800 μl medium containing 10% FBS were respectively added into the top chamber and the bottom chamber. After 36 h of treatment, the cells were then stained with 0.1% crystal violet for 30 min, and non-migrated cells were removed. Ten visual fields were randomly chosen to calculate the number of migrated cells.

### 2.12. Statistical analyses

Results are expressed as mean ± S.E.M. Student's t-test and one-way analysis of variance (ANOVA) were performed to analyze differences between experimental groups. $P < 0.05$ was considered statistical significance. Graphical results were analyzed using GraphPad Prism 8 (GraphPad Software, Inc., La Jolla, CA, USA). All the experiments were replicated three times at least.

## 3. Results

### 3.1. HG/HF stress causes dysfunction of HUVECs in a concentration-dependent manner

As shown in Fig. 1, the results of H & E staining displayed that the cell number and morphology in low concentration groups such as 11/0.125 and 22/0.25 mM had little difference compared with those in Control group, presenting cell confluency was high and cells were evenly distributed. However, with the increase of HG/HF concentration, the number of cells began to decrease, and the morphology gradually became wrinkled, shortened, and even ruptured (Fig. 1A). As expected, with the concentration of HG/HF increased, the reactive oxygen species levels denoted by DCF fluorescence intensity increased gradually, and reached to a maximum at 55/2.0 mM (Fig. 1B and C). Besides, the cell viability assay also found that higher concentrations of HG/HF markedly reduced the cell viability. Moreover, the higher is the concentration, the lower is the cell viability (Fig. 1D). Western blotting results further exhibited that the levels of NO and p-eNOS had no significant difference at low concentration of HG/HF (11/0.125 mM) compared with Control group. However, with the concentration of HG/HF elevated, the levels of NO and p-eNOS gradually decreased in a concentration-dependent manner (Fig. 1E and F).

### 3.2. HG/HF stress induces autophagy in a concentration- and time-dependent manner

Then, we sought to investigate the relationship between the HG/HF

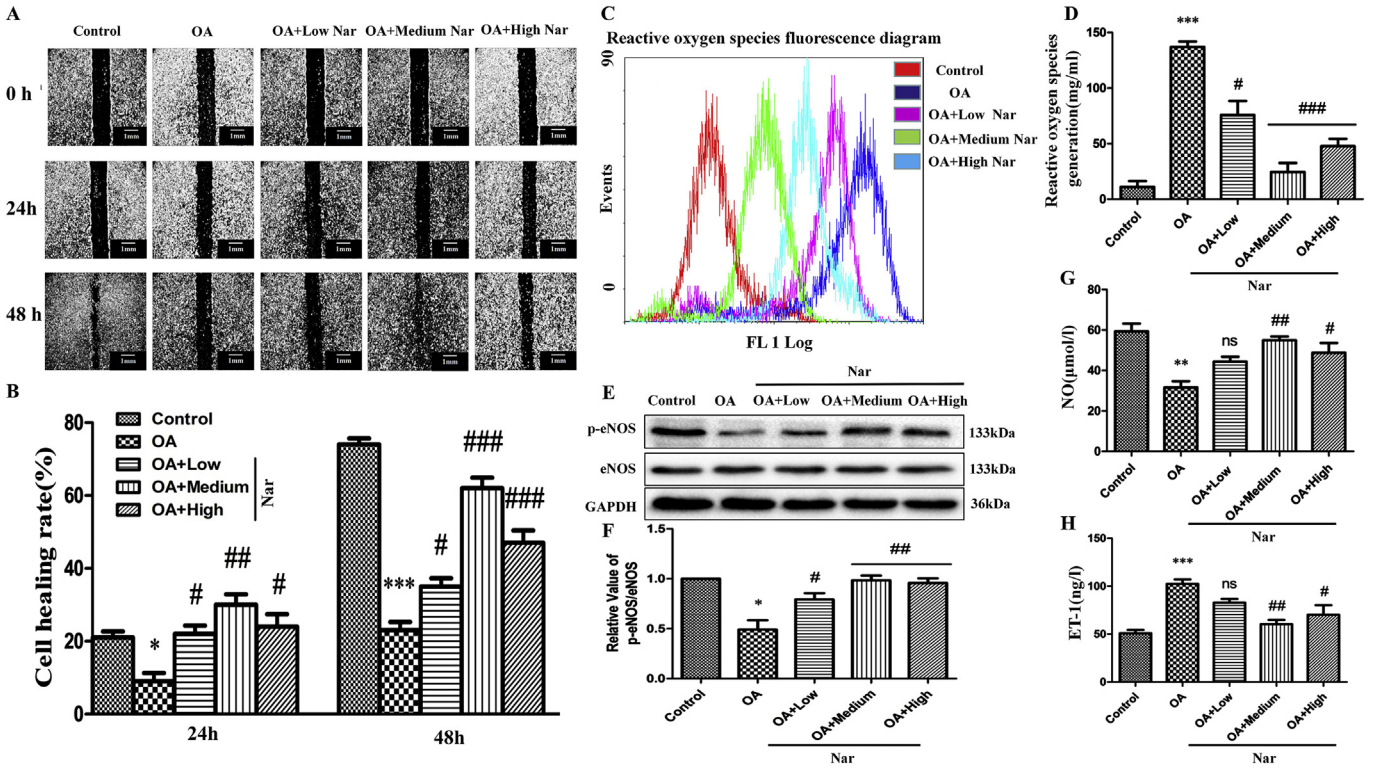


**Fig. 3.** Nar protects HUVECs against dysfunction induced by HG/HF stress. 95% confluent HUVECs were exposed to the indicated glucose/palmitic acid (PA) concentration combinations including Control (5.5/0 mM) and 44/1.0 mM of HG/HF for 24 h (optimal autophagy, OA), and then the HG/HF-treated cells were respectively treated with 43 μM (Low), 86 μM (Medium) and 172 μM (High) of Nar for another 24 h. Finally, cell healing function (A and B), reactive oxygen species generation (C and D) and p-eNOS levels in cells (E and F), NO (G) and ET-1 levels (H) in supernatant were detected. GAPDH was considered as a loading control. Data are expressed as mean ± S.E.M. of 3 independent experiments. Student's t-test and ANOVA were performed. $^{*}P < 0.05$, $^{**}P < 0.01$, $^{***}P < 0.001$, *vs.* Control group; $^{\#}P < 0.05$, $^{\#\#}P < 0.01$, $^{\#\#\#}P < 0.001$ *vs.* OA group; ns: no significant difference. p-eNOS: phosphorylated endothelial NO synthase, ET-1: endothelin 1, HG/HF: high glucose/high fat, Nar: Naringin, NO: nitric oxide, OA: optimal autophagy condition (44/1.0 mM of HG/HF for 24 h). Scale bar in A: 1 mm.

stress and autophagy. Our results showed that with the gradual increase of HG/HF concentration, the ratio of LC3-II to LC3-I and the Beclin 1 levels presented an upward trend, while the p62 levels were just opposite to the ratio of LC3-II to LC3-I and the Beclin 1 levels (Fig. 2A–D), indicating that the HG/HF stress induced autophagy in a concentration-dependent manner. Moreover, we wondered the time course of the HG/HF stress-induced autophagy. The results showed that the ratio of LC3-II to LC3-I and the Beclin1 was increased significantly from 24 h to 60 h while the p62 levels was decreased (Fig. 2E–H), indicating that the HG/HF stress induced autophagy in a certain time-dependent manner. Taken together, based on the effects of HG/HF on the viability, function and autophagy levels, we chose the 44/1.0 mM and the 24 h as the optimal autophagy (OA)-induced condition of HG/HF. Subsequently, under such an OA condition, we visualized the autophagosomes by the MDC staining. Our results displayed that compared with the Control group, the green fluorescent intensity of the OA group was stronger than that of control group (Fig. 2I), indicating that the HG/HF stress indeed induced autophagy.

### 3.3. Nar improves the function of HUVECs under HG/HF stress

To investigate the effect of Nar on the function of HUVECs under the HG/HF stress, the experiment was designed into Control, OA, OA + low (43 μM), medium (86 μM),and high concentration (172 μM) Nar groups, respectively. The results showed that the cells in OA group proliferated and migrated more slowly than those in Control group whereas treatment with Nar normalized the cell proliferation and migration, especially the medium concentration of Nar (Fig. 3A and B). Besides, the reactive oxygen species results displayed that Nar antagonized the over-production of reactive oxygen species induced by HG/HF stress (Fig. 3C and D). The results of the p-eNOS and NO levels also exhibited Nar reversed the fall in the p-eNOS and NO levels induced by HG/HF stress (Fig. 3E–G). Our results revealed that the HG/HF stress markedly elevated the ET-1 levels whereas Nar counteracted the elevation of ET-1 induced by the HG/HF stress (Fig. 3H).

### 3.4. Nar inhibits autophagy of HUVECs induced by HG/HF stress

We analyzed the levels of autophagy-related proteins under HG/HF stress in the presence of Nar. Our results showed that the ratio of LC3-II to LC3-I was decreased significantly both in the OA + medium concentration and OA + high concentration Nar group, while there was no significant difference between OA and OA + low concentration Nar group (Fig. 4A and B). The expression levels of Beclin1 were similar to those of the ratio of LC3-II to LC3-I (Fig. 4A and D). However, the expression levels of p62 increased with the elevation of Nar concentration (Fig. 4A and C). Subsequently, we selected the medium concentration of Nar for 24 h as the optimal Nar-treatment condition (ON) to detect LC3 immunofluorescence and MDC staining in OA and OA + ON group. The results showed that both LC3 protein and the number of autophagosome in the OA + ON group were significantly lower than those in the OA group (Fig. 4E), indicating that Nar represses the autophagy induced by the HG/HF stress.

### 3.5. Nar ameliorates dysfunction of HUVECs induced by HG/HF stress by inhibiting autophagy

We next wonder whether the dysfunctional improvement of Nar is fulfilled by inhibiting autophagy induced by HG/HF stress. As shown in Fig. 5, the cell migration assay results showed treatment with 86 μM of

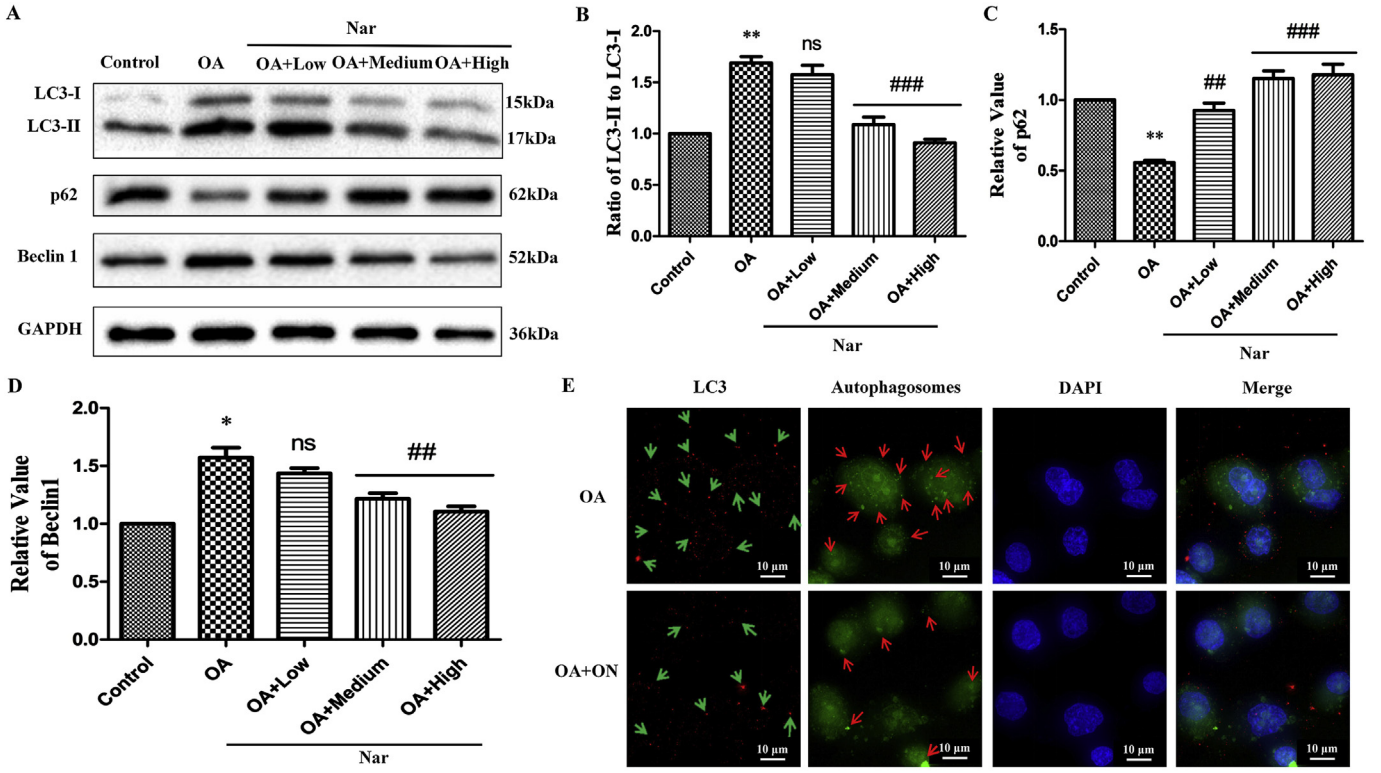


**Fig. 4.** Nar inhibits autophagy of HUVECs induced by HG/HF stress. 95% confluent HUVECs were exposed to the indicated glucose/palmitic acid (PA) concentration combinations including Control (5.5/0 mM) and 44/1.0 mM of HG/HF for 24 h (optimal autophagy, OA), and then the HG/HF-treated cells were respectively treated with 43 μM (Low), 86 μM (Medium) and 172 μM (High) of Nar for another 24 h. The levels of LC3-II/LC3-I (A and B), p62 (A and C) and Beclin1 (A and D) were determined by western blotting and the autophagosomes were visualized by MDC staining (E). GAPDH was considered as a loading control. Data are expressed as mean ± S.E.M. of 3 independent experiments. Student's t-test and ANOVA were performed. $^{*}P < 0.05$, $^{**}P < 0.01$, *vs.* Control group; $^{\#\#}P < 0.01$, $^{\#\#\#}P < 0.001$ *vs.* OA group; ns: no significant difference; HG/HF: high glucose/high fat, MDC: mondansylcadaverin (a fluorescent dye forautophagosome), Nar: Naringin, OA: optimal autophagy condition (44/1.0 mM of HG/HF for 24 h). Scale bar in E: 10 μm.

Nar (OA + ON) significantly elevated the cell migration level compared with OA group. However, the treatment combined with 86 μM of Nar and 5 μM of RAPA (OA + ON + RAPA) notably reversed the elevation triggered by Nar, whereas the treatment combined with 86 μM of Nar and 2.5 mM of 3-MA (OA + ON+3-MA) considerably increased the elevation triggered by Nar, demonstrating that the Nar-pro-migration was owing to inhibiting autophagy (Fig. 5A–C). Similarly, the LDH activity results demonstrated the protective effect of Nar against the injury of HUVEC was also attributed to autophagy inhibition (Fig. 5D).

### *3.6. Nar inhibits excessive autophagy induced by HG/HF stress by activating PI3K-Akt-mTOR pathway*

Finally, molecular mechanisms of Nar-inhibiting excessive autophagy to improve cell function were explored. The results showed the expression levels of p-PI3K, p-Akt and p-mTOR in OA + ON group were increased significantly compared with those of OA group (Fig. 6A–D). These data suggested that Nar activated the PI3K-Akt-mTOR pathway. To further confirm the causal relation between autophagy and the PI3K-Akt-mTOR pathway activated by Nar, both 10 μM LY294002 (PI3K inhibitor) and 0.5 μM Akt inhibitor IV (Akt inhibitor) were used and the autophagy markers were detected by western blotting. The results showed that the ratio of LC3-II to LC3-I and the expression level of Beclin1 were significantly increased while the expression level of p62 was significantly decreased in the presence of either LY294002 or Akt inhibitor IV, indicating that inhibition of this pathway rescued the decrease of autophagy induced by Nar and further demonstrating Nar acted to inhibit autophagy by activating the pathway. Moreover, the expression levels of p-eNOS in OA + ON + LY294002 group and OA + ON + Akt inhibitor IVgroup were significantly lower than those in OA + ON group, suggesting that treatment with either LY294002 or Akt inhibitor IV expedited the decrease in p-eNOS levels (Fig. 6E–I). The reactive oxygen species results showed that the reactive oxygen species levels either in the OA + ON + LY294002 group or the OA + ON + Akt inhibitor IV group was significantly higher than that in the OA + ON group (Fig. 6J and K), further confirming that Nar improved cell function by activating the PI3K-Akt-mTOR pathway.

## 4. Discussion

Given glucose and lipids are necessary nutrients to our daily diet, the experiment combines glucose and lipid to establish the cell injury model induced by HG/HF (Tobias et al., 2014; Hoch et al., 2015). In adult human, the normal glycemia is 3.89–6.11 mmol/l, the normal total cholesterol is 2.8–5.17 mmol/l and the triglyceride is 0.56–1.7 mmol/l (Scholte et al., 2011). The HG/HF concentration levels used in this study were above the upper threshold values.

The morphology and quantity of cells plays a very important role in maintaining cell function (Pernagallo et al., 2008). However, HG/HF changes the cell morphology and quantity, which in turn affects cell function. Studies have shown that the function of cell was inhibited after prolonged exposure to HG/HF (Fu et al., 2017). Thus, we first aimed to determine the alterations in cell morphology and quantity that occur during HG/HF stress. The results of H&E staining displayed that HG/HF changed the morphology and quantity of cells, suggesting that HG/HF manifested notable gluco-toxicity and lipid-toxicity to cells. We next considered the markers to evaluate the endothelial function. It is well known that the eNOS/NO signaling plays a critical role in vascular patho-physiological process. The eNOS exclusively distributes in vascular endothelial cells and it is essential for the synthesis of endothelial

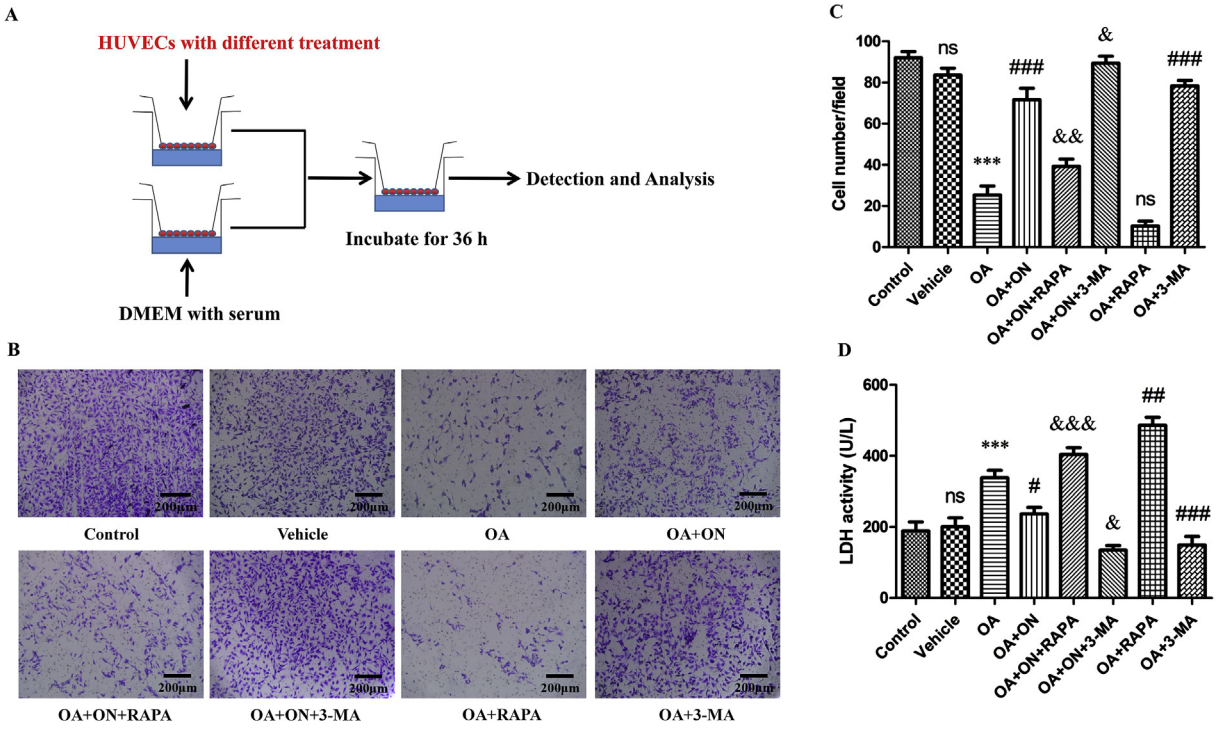


**Fig. 5.** Nar ameliorates dysfunction of HUVECs induced by HG/HF stress by inhibiting autophagy. 95% confluent HUVECs were exposed to the indicated glucose/palmitic acid (PA) concentration combinations including Control (5.5/0 mM), Vehicle (DMSO) and 44/1.0 mM of HG/HF for 24 h (optimal autophagy, OA), and then the HG/HF-treated cells were divided into two batches; one batch of the cells were treated with either 86 μM Nar (OA + ON) or 5 μM RAPA (OA + RAPA) or 2.5 mM 3-MA (OA + 3-MA) for another 24 h, and the other were treated by 86 μM Nar combined either with 5 μM RAPA (OA + ON + RAPA) or 2.5 mM 3-MA (OA + ON + 3-MA) for additional 24 h. Finally, all these cells were used to detect migration function by a trans-well assay (A, B, C) and the supernatant was used to measure the LDH activity (D). 'A' diagram shows a workflow of the trans-well assay. 'B' images display the migrated and infiltrated cells by Crystal purple staining and 'C' histograph shows the migrated and infiltrated cell numbers. Data are expressed as mean ± S.E.M. of 3 independent experiments. Student's t-test and ANOVA were performed. $^{***}P < 0.001$, *vs.* Control group; $^{\#}P < 0.05$, $^{\#\#}P < 0.01$, $^{\#\#\#}P < 0.001$ *vs.* OA group; $^{\&}P < 0.05$, $^{\&\&}P < 0.01$, $^{\&\&\&}P < 0.001$ *vs.* OA + ON group; ns: no significant difference. HG/HF: high glucose/high fat, LDH: lactate dehydrogenase, 3-MA: 3-methyladenine (an inhibitor of autophagy), Nar: Naringin, OA: optimal autophagy condition (44/1.0 mM of HG/HF for 24 h), ON: optimal condition of Nar, RAPA: rapamycin (an inducer of autophagy). Scale bar in B: 200 μm.

NO (Pearce and Pearce, 2013). Erdogan et al. found that NO, as an endothelium-derived relaxing factor, activates soluble guanylate cyclase and relaxes vascular smooth muscle by increasing the levels of cyclic guanosine monophosphate (Erdogan et al., 2018). It is believed that oxidative stress has an effect on endothelial cell injury. A large number of studies have demonstrated that endothelial cell injury induced by hyperglycemia and/or hyperlipidemia is owing to oxidative stress mediated by reactive oxygen species (Dijkstra et al., 1998; Hsueh et al., 2016; Li et al., 2015). In the endothelial cells, the intracellular reactive oxygen species including superoxide anion, hydrogen peroxide and hydroxyl radical is primarily derived from the oxidation-phosphorylation of glucose and fatty acids in mitochodria, especially under the condition of hyperglycemia and hyperlipidemia. By measuring these indexes, we can assess the state of endothelial cell function. Our results showed that these indexes altered after HG/HF treatment, and then we concluded that the HG/HF stress disturbed the endothelial cell function. Of course, we realized that lower concentrations of glucose and palmitic acid are used as nutrients to promote cell survival and maintain cellular function, whereas higher concentrations injure cells. These results are consistent with our previous results (Zhang et al., 2015).

Growing evidence showed that autophagy occurs under some physiological conditions and it plays important roles in cell survival and homeostasis. For example, in the case of hunger, due to the lack of nutrients, autophagy occurs in many organs such as liver, spleen, kidney, etc. Chen et al. found that autophagy protects spinal cord neurons against mechanical injury (Chen et al., 2012). Torres et al. also found that autophagy could promote vascular endothelial cell migration (Torres et al., 2017). Consequently, moderate autophagy is a protective adaptive process (Rabinowitz and White, 2010). However, excessive autophagy and/or blockade of autophagy flux can lead to autophagic dysfunction, which is considered one of the causes of cell damage and even death. Research has shown that exposure to the environmental lead increases the activation of autophagy and leads to autophagic death in rat hippocampus (Sutton et al., 2018). It has been reported that 2, 5-hexanedione can over-activate autophagy in VSC4.1 cells, resulting in autophagic death of VSC4.1 cells (Guan et al., 2017). Inhibition of the autophagic flow of H9c2 cardiomyocytes results in abnormal accumulation of autophagosomes, which promotes cardiomyocyte apoptosis and finally leads to myocardial cell damage (Zhang et al., 2016). Nevertheless, at present, it is largely unknown whether autophagy occurs in the case of HG/HF stress in the endothelial cells. Therefore, in this study, we investigated the relationship between the HG/HF stress and autophagy. In the present study, the ratio of LC3-II to LC3-I combined with the p62 levels were used to evaluate the autophagy levels (Mitroi et al., 2017). In addition, Beclin1 promotes the localization of other autophagy-related proteins in the autophagosomes to increase autophagy activity or to activate autophagy (Masuda et al., 2016; Valente et al., 2014). Our results confirm that the HG/HF stress significantly induces autophagy in HUVECs by detecting the expression levels of these autophagy-related proteins.

In general, autophagy occurs in hunger and cold so on. Nutrients such as glucose, amino acids and fatty acids inhibit autophagy (Cuervo and Macian, 2012). However, in this study, we obtained seemingly contradictory results. As for the likely reasons, in our opinion, there might be two aspects at least. One is the cell specificity. For example, cardiomyocytes are distinct from endothelial cells and adipocytes in response to nutrient stress (Gangaiah et al., 2016). The other is that the

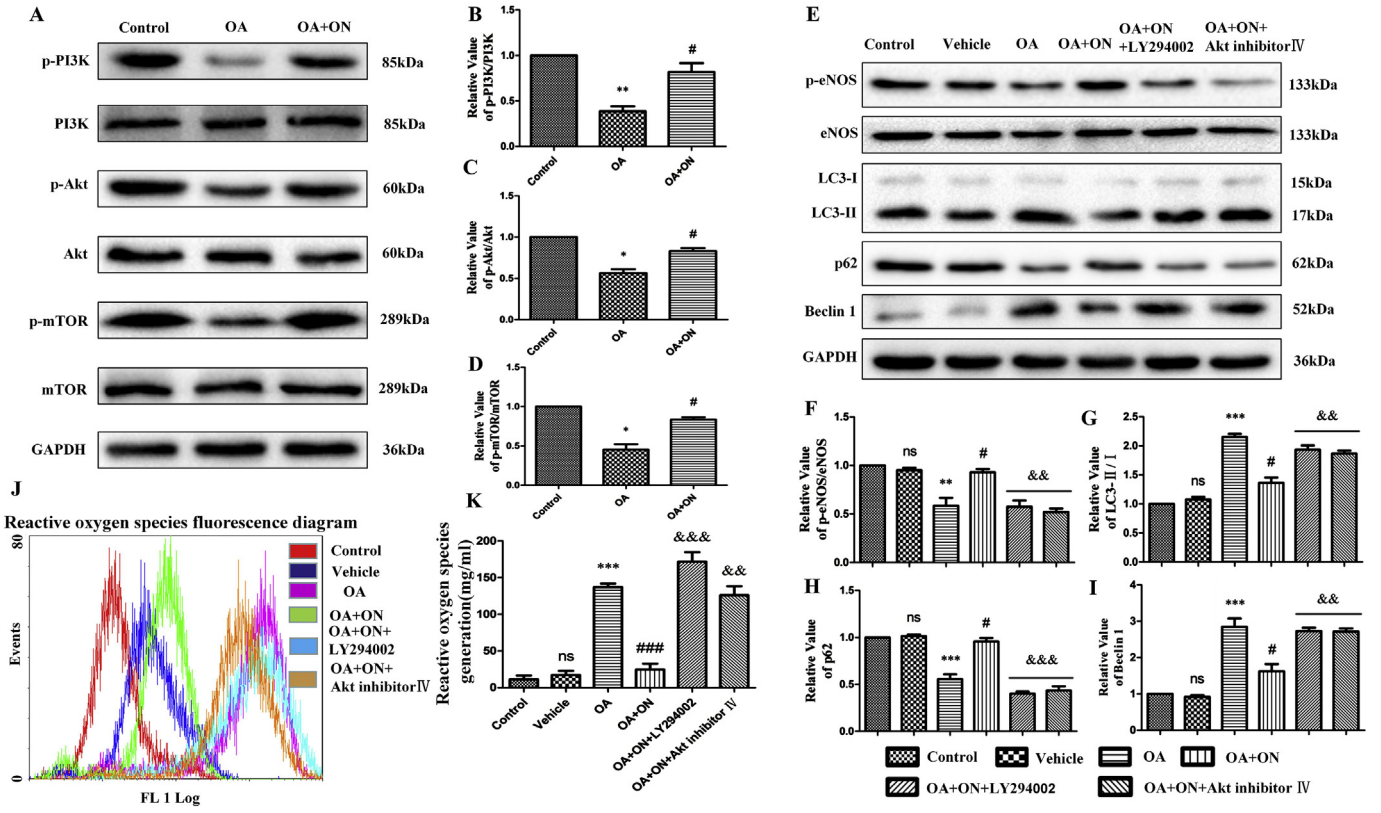


**Fig. 6.** Nar inhibits excessive autophagy induced by HG/HF stress by activating PI3K-Akt-mTOR pathway. 95% confluent HUVECs were exposed to various glucose/palmitic acid (PA) concentration combinations including Control (5.5/0 mM) and 44/1.0 mM of HG/HF for 24 h (optimal autophagy, OA), and then the HG/HF-treated cells were divided into two batches; one batch of the cells were treated with either 86 μM Nar (OA + ON) for another 24 h, and the other were treated by 86 μM Nar combined with either 10 μM LY294002 or 0.5 μM Akt inhibitor IV or vehicle for additional 24 h. Finally, the levels of p-PI3K, p-Akt and p-mTOR were determined by western blotting (A–D) and the levels of p-eNOS, LC3-II/LC3-I, p62 and Beclin1 were determined by western blotting (E–I). The generation of reactive oxygen species was measured by flow cytometry (J and K). Data are expressed as mean ± S.E.M. of 3 independent experiments. Student's t-test and ANOVA were performed. $^{*}P < 0.05$, $^{**}P < 0.01$, $^{***}P < 0.001$, *vs.* Control group; $^{\#}P < 0.05$, $^{\#\#\#}P < 0.001$ *vs.* OA group; $^{\&\&}P < 0.01$, $^{\&\&\&}P < 0.001$ *vs.* OA + ON group; ns: no significant difference. Akt inhibitor VI: an Akt inhibitor, p-eNOS: phosphorylated endothelial NO synthase, HG/HF: high glucose/high fat, LY294002: a PI3K inhibitor, Nar: Naringin, OA: optimal autophagy condition (44/1.0 mM of HG/HF for 24 h), ON: optimal condition of Nar.

response of cells to different doses of nutrients is different (Newsholme et al., 2014). At a lower dose, cells can fully utilize these nutrients to provide ATP, and the level of autophagy is low. However, at a higher dose, cells regard the surplus nutrients as exotic substances to be eliminated and thus the autophagy is activated or enhanced. As a result, the normal components of the cells were also phagocytized, eventually leading to cell damage.

It has been reported that flavonoids have preventive and therapeutic effects in cardiovascular diseases and diabetic complications (Kumar et al., 2016). Jia et al. found that flavonoids extracted from lagerstroemia speciosa could alleviate HUVECs injury induced by hydrogen peroxide (Jia et al., 2012). In addition, Nar is a dihydroflavone compound with obvious pharmacological effects such as anti-inflammation, anti-oxidation, improving insulin resistance, regulating glycolipid metabolism, etc. However, whether Nar could improve endothelial cell function under HG/HF stress is still unclear. In the study, we investigated the changes of cell function including proliferation and migration as well as endocrine after treatment with Nar. Our present results demonstrate that Nar reverses the decreases of cell function induced by HG/HF stress, which is consistent with the results of other studies (Park et al., 2018; Ma et al., 2016). However, compared with the low concentration and high concentration of Nar, the medium concentration of Nar is seemingly better for improving cell function under HG/HF stress. As for the reason, we can obtain the plausible explanation from the bioavailability and metabolism of Nar. When administered orally, Nar is suffered from de-glycosylation prior to absorption through the intestinal epithelium, and then undergone metabolism by phase II conjugating enzymes, thus resulting in the circulating Nar metabolite levels being in the nM range (Zeng et al., 2016). Therefore, the low concentration of Nar does not reach the threshold concentration, while the high concentration exceeds that of the maximal efficacy which likely leads to a little toxicity. Taken together, our data validated that Nar ameliorates the dysfunction of endothelial cells induced by HG/HF stress.

Several studies have demonstrated that flavonoids induce autophagy in some physiological processes (Prieto-Domínguez et al., 2018; Kim et al., 2016). However, another study has displayed that flavonoids exert anti-tumor effects through autophagy inhibition (Chakrabarti et al., 2015). Therefore, in this study, we sought to investigate the effects of Nar on autophagy levels induced by HG/HF stress. Our present results displayed that Nar can inhibit autophagy induced by the HG/HF stress.

The mTOR is thought to be an important homeostatic regulator of cell growth, proliferation, survival and metabolism by up-regulating protein, lipid synthesis and inhibiting excessive autophagy (Cuervo and Macian, 2012). RAPA activates autophagy by inhibiting mTOR but 3-MA inhibits autophagy by activating mTOR (Nakatsu et al., 2010). Since the results described above have demonstrated that Nar improves the dysfunction and inhibits autophagy induced by HG/HF stress, we next wonder whether the dysfunction improvement of Nar is fulfilled by inhibiting autophagy induced by HG/HF stress. To address this issue, RAPA and 3-MA were utilized. Our present results ascertained that Nar

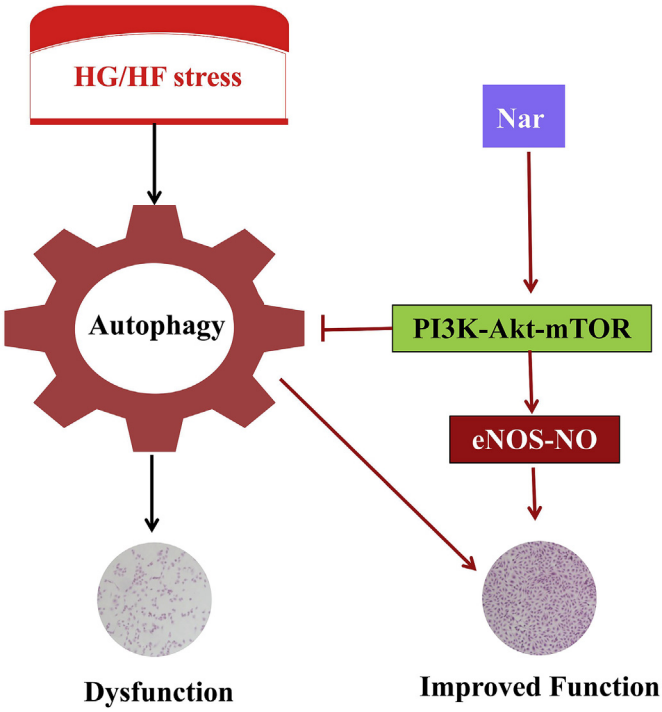


**Fig. 7.** Schematic for a putative working model of Nar. HG/HF stress results in autophagy of endothelial cells, which damages morphology, and function. Nar activates PI3K-Akt-mTOR pathway to inhibit cell autophagy and to activate eNOS-NO signaling, thus improving cell function.

improves cell function by inhibiting autophagy because re-activation of autophagy by RAPA reverses the protective effects of Nar against dysfunction whereas 3-MA amplifies the Nar-protective effects. Accordingly, we also concluded HG/HF stress causes cell dysfunction by inducing cell excessive autophagy.

It is well known that the PI3K-Akt-mTOR pathway regulates a variety of cellular processes, including apoptosis, proliferation, metabolism et al. (Heras-Sandoval et al., 2014; Fabre et al., 2005; Zabala-Letona et al., 2017). It is reported that IL-37 induces autophagy in hepatoma cells by inhibiting the PI3K-Akt-mTOR pathway (Li and Zhu et al., 2017). Autophagy is involved in melanin degradation induced by heterooligonucleotides in human epidermal keratinocytes by PI3K-Akt-mTOR signaling (Yang et al., 2018). Our results indicate that Nar has an activation effect on the PI3K-Akt-mTOR pathway that can be demonstrated from the expression levels of their phosphorylated proteins. Furthermore, PI3K inhibitor and Akt inhibitor can abolish the effect of Nar on autophagy, further demonstrating that Nar activates the PI3K-Akt-mTOR pathway to inhibit autophagy, thereby improving the damage of HUVECs. Our data have indicated that Nar inhibits autophagy by activating the PI3K-Akt-mTOR pathway to ameliorate endothelial cell dysfunction induced by HG/HF stress. As for the mechanisms responsible for Nar-normalizing NO and ET-1 levels and the relation between autophagy and normalization of NO and ET-1 levels, our results have clearly shown that Nar activates the PI3K-Akt-mTOR pathway. The activation of PI3K-Akt-mTOR pathway by Nar, on one hand, inhibits excessive autophagy induced by HG/HF stress, and on the other hand, it activates the eNOS/NO signaling and thus resulting in normalization of NO and ET-1 levels.

## 5. Conclusion

Our present study first demonstrated that Nar reverses HG/HF stress-induced autophagic dysfunction in HUVECs by activating the PI3K-Akt-mTOR pathway. Moreover, we have proposed that glycolipids have different effects on autophagy at different concentrations and Nar alleviates the damage of HUVECs and improves the dysfunction induced by HG/HF stress by inhibiting autophagy (Fig. 7). The findings offer an insight into HG/HF stress-induced autophagy and indicate that as a drug-food dual compound, Nar might have potential to prevent and treat the diabetic angiopathy. Of course, the data is only from in vitro experiments, and the in vivo experiments will be further performed in the future.

## Author contributions

Qiren Huang: Conceptualization, Methodology, Formal analysis, Writing- Reviewing and Editing. Kun Wang: Investigation, Writing-Original draft preparation, Visualization. Shengjia Peng: Investigation, Validation, Formal analysis. Shaofeng Xiong: Validation. Ailin Niu: Software. Min Xia: Data curation. Xiaowei Xiong: Project administration. Guohua Zeng: Supervision, Validation.

## Declaration of competing interest

There are no conflicts of interest to declare.

## Acknowledgements

We acknowledge the support from the National Natural Science Foundation of China (31660323, 81960153, 30860111, 81070633, 81360060) and Jiangxi Provincial Department of Science & Technology (20123BCB22005). We also acknowledge the support from the National College Students Innovation and Entrepreneurship Training Program (201910403018). We are also very grateful to Prof. Lu Guizhen (Peking Union Medical College Central Laboratory, CHN), who generously provided us the high-resolution live cell imaging system Deltavision$^{TM}$Ultra.

## References

Xu, Q., Zhang, Z.F., Sun, W.X., 2017. Effect of naringin on monosodium iodoacetate-induced osteoarthritis pain in rats. Med. Sci. Mon. Int. Med. J. Exp. Clin. Res. 23, 3746–3751. https://doi.org/10.12659/msm.902396.

Chakrabarti, M., Ai, W., Ray, S.K., 2015. Abstract 1010: synergistic antitumor effects of luteolin and silibinin with overexpression of miR-7-1-3p inhibited autophagy and promoted apoptosis in glioblastoma. Canc. Res. 75 (15), 1207–1213. https://doi.org/10.1158/1538-7445.AM2015-1010.

Chen, H.C., Fong, T.H., Lee, A.W., Chiu, W.T., 2012. Autophagy is activated in injured neurons and inhibited by methylprednisolone after experimental spinal cord injury. Spine 37 (6), 470–475. https://doi.org/10.1097/brs.0b013e318221e859.

Chen, R.C., Sun, G.B., Wang, J., Zhang, H.J., Sun, X.B., 2015. Naringin protects against anoxia/reoxygenation-induced apoptosis in H9c2 cells via the Nrf2 signaling pathway. Food Funct 6 (4), 1331–1344. https://doi.org/10.1039/C4FO01164C.

Cuervo, A.M., Macian, F., 2012. Autophagy, nutrition and immunology. Mol. Aspect. Med. 33 (1). https://doi.org/10.1016/j.mam.2011.09.001. 0-13.

Dey, N., De, P., Leyland-Jones, B., 2017. PI3K-AKT-mTOR inhibitors in breast cancers: from tumor cell signaling to clinical trials. Pharmacol. Therapeut. 175, 91–106. https://doi.org/10.1016/j.pharmthera.2017.02.03.

Dijkstra, G., Moshage, H., Dullemen, H.M.V., Jager-Krikken, A.D., Tiebosch, A.T., Kleibeuker, J.H., Jansen, P.L., Goor, H., 1998. Expression of nitric oxide synthases and formation of nitrotyrosine and reactive oxygen species in inflammatory bowel disease. J. Pathol. 186 (4), 416–421. https://doi.org/10.1002/(SICI)1096-9896(199812)186:43.0.CO;2-U.

Erdogan, M., Kulaksizoglu, M., Tetik, A., Solmaz, S., Kucukaslan, A.S., Eroglu, Z., 2018. The relationship of the endothelial nitric oxide synthase (eNOS) and vascular endothelial growth factor (VEGF) gene polymorphism in Turkish type 2 diabetic patients with and without diabetic foot ulcers. Foot 37, 5–10. https://doi.org/10.1016/j.foot.2018.06.006.

Fabre, S., Lang, V., Harriague, J., Jobart, A., Unterman, T.G., Trautmann, A., Bismuth, G., 2005. Stable activation of phosphatidylinositol 3-kinase in the T cell immunological synapse stimulates Akt signaling to Foxo1 nuclear exclusion and cell growth control. J. Immunol. 174 (7), 4161–4171. https://doi.org/10.4049/jimmunol.174.7.4161.

Fu, J.Q., Cui, Q., Yang, B., Hou, Y.Y., Wang, H.H., Xu, Y.Y., Wang, D.F., Zhang, Q., Pi, J.B., 2017. The impairment of glucose-stimulated insulin secretion in pancreatic β-cells caused by prolonged glucotoxicity and lipotoxicity is associated with elevated adaptive antioxidant response. Food Chem. Toxicol. 100, 161–167. https://doi.org/10.1016/j.fct.2016.12.016.

Gangaiah, D., Zhang, X., Baker, B., Fortney, K.R., Gao, H., Holley, C.L., Munson, R.S., Liu, Y., Spinola, S.M., 2016. Haemophilus ducreyi seeks alternative carbon sources and adapts to nutrient stress and anaerobiosis during experimental infection of human

volunteers. Infect. Immun. 84 (5), 1514–1525. https://doi.org/10.1128/IAI.00048-16.
Guan, H., Piao, H., Qian, Z., Zhou, X., Sun, Y., Cao, C., Li, S., Piao, F., 2017. 2,5-Hexandeione induces autophagic death of VSC4.1 cells via a PI3K/Akt/mTOR pathway. Mol. Biosyst. 13 (10), 1993–2005. https://doi.org/10.1039/C7MB00001D.
Heras-Sandoval, D., Pérez-Rojas, J.M., Hernández-Damián, J., Pedraza-Chaverri, J., 2014. The role of PI3K/AKT/mTOR pathway in the modulation of autophagy and the clearance of protein aggregates in neurodegeneration. Cell. Signal. 26 (12), 2694–2701. https://doi.org/10.1016/j.cellsig.2014.08.01.
Hoch, T., Kreitz, S., Gaffling, S., Pischetsrieder, M., Hess, A., 2015. Fat/carbohydrate ratio but not energy density determines snack food intake and activates brain reward areas. Sci. Rep. 5, 10041. https://doi.org/10.1038/srep10041.
Hsueh, T.P., Sheen, J.M., Pang, J.H., Bi, K.W., Huang, C.C., Wu, H.T., Huang, S.T., 2016. The anti-atherosclerotic effect of naringin is associated with reduced expressions of cell adhesion molecules and chemokines through NF-κB Pathway. Molecules 21 (2), 195. https://doi.org/10.3390/molecules21020195.
Jia, Y.N., Ji, L., Zhang, S., Xu, L., Yin, L.H., Li, L., Zhao, Y.Y., Peng, J.Y., 2012. Total flavonoids from Rosa Laevigata Michx fruit attenuates hydrogen peroxide induced injury in human umbilical vein endothelial cells. Food Chem. Toxicol. 50 (9), 3133–3141. https://doi.org/10.1016/j.fct.2012.06.047.
Karuna, R., Holleboom, A.G., Motazacker, M.M., Kuivenhoven, J.A., Frikke-Schmidt, R., Tybjaerg-Hansen, A., Georgopoulos, S., Miranda, E., ckf Berkel, T., Eckardstein, A., Rentsch, K.M., 2011. Plasma levels of 27-hydroxycholesterol in humans and mice with monogenic disturbances of high density lipoprotein metabolism. Atherosclerosis 214 (2), 448–455. https://doi.org/10.1016/j.atherosclerosis.2010.10.042.
Kim, I.R., Kim, S.E., Baek, H.S., Kim, B.J., Kim, C.H., Chuang, I.K., Park, B.S., Shin, S.H., 2016. The role of kaempferol-induced autophagy on differentiation and mineralization of osteoblastic MC3T3-E1 cells. BMC Compl. Alternative Med. 16 (1), 333. https://doi.org/10.1186/s12906-016-1320-9.
Kulasekaran, G., Ganapasam, S., 2015. Neuroprotective efficacy of naringin on 3-nitropropionic acid-induced mitochondrial dysfunction through the modulation of Nrf2 signaling pathway in PC12 cells. Mol. Cell. Biochem. 409 (1–2), 199–211. https://doi.org/10.1007/s11010-015-2525-9. doc:.
Kumar, M.P., Raju, T.N., Naik, R.R., 2016. The preventive effect of flavonoids on aldose reductase and protein glycation in diabetic complications. Cardiovasc. Hematol. Agents Med. Chem. 14 (999). https://doi.org/10.2174/1871525714666160518121346. 1-1.
Lamoureux, F., Zoubeidi, A., 2013. Dual inhibition of autophagy and the AKT pathway in prostate cancer. Autophagy 9 (7), 1119–1120. https://doi.org/10.4161/auto.24921.
Lavrador, P., Gaspar, V.M., Mano, J.F., 2018. Bioinspired bone therapies using naringin: applications and advances. Drug Discov. Today 23 (6), 1293–1304. https://doi.org/10.1016/j.drudis.2018.05.012.
Li, L.L., Tan, J., Miao, Y.Y., Lei, P., Zhang, Q., 2015. ROS and autophagy: interactions and molecular regulatory mechanisms. Cell. Mol. Neurobiol. 35 (5), 615–621. https://doi.org/10.1007/s10571-015-0166-x.
Li, T.T., Zhu, D., Mou, T., Guo, Z., Pu, J.L., Chen, Q.S., Wei, X.F., Wu, Z.J., 2017. IL-37 induces autophagy in hepatocellular carcinoma cells by inhibiting the PI3K/AKT/mTOR pathway. Mol. Immunol. 87, 132–140. https://doi.org/10.1016/j.molimm.2017.04.010.
Li, Y., Lu, L., Luo, N., Wang, Y.Q., Gao, H.M., 2017. Inhibition of PI3K/AKt/mTOR signaling pathway protects against d-galactosamine/lipopolysaccharide-induced acute liver failure by chaperone-mediated autophagy in rats. Biomed. Pharmacother. 92, 544–553. https://doi.org/10.1016/j.biopha.2017.05.037.
Ma, X., Lv, J., Sun, X., Ma, J., Xing, G., Wang, Y., Sun, L., Wang, J., Li, F., Li, Y., Zhao, Z., 2016. Naringin ameliorates bone loss induced by sciatic neurectomy and increases Semaphorin 3A expression in denervated bone. Sci. Rep. 6 (1), 24562. https://doi.org/10.1038/srep24562.
Masuda, G.O., Yashiro, M., Kitayama, K., Miki, Y., Kasashima, H., Kinoshita, H., Morisaki, T., Fukuoka, T., Hasegawa, T., Sakurai, K., Toyokawa, T., Kubo, N., Tanaka, H., Hirakawa, K., 2016. Clinicopathological correlations of autophagy-related proteins LC3, Beclin 1 and p62 in gastric cancer. Anticancer Res. 36 (1), 129–136.
Mitroi, D.N., Karunakaran, I., Gräler, M., Saba, J.D., Ehninger, D., Ledesma, M.D., van Echten-Deckert, G., 2017. SGPL1 (sphingosine phosphate lyase 1) modulates neuronal autophagy via phosphatidylethanolamine production. Autophagy 13 (5), 885–899. https://doi.org/10.1080/15548627.2017.1291471.
Nakatsu, Y., Kotake, Y., Takai, N., Ohta, S., 2010. Involvement of autophagy via mammalian target of rapamycin (mTOR) inhibition in tributyltin-induced neuronal cell death. J. Toxicol. Sci. 35 (2), 245–251. https://doi.org/10.2131/jts.35.245.
Newsholme, P., Cruzat, V., Arfuso, F., Keane, K., 2014. Nutrient regulation of insulin secretion and action. J. Endocrinol. 221 (3), R105–R120. https://doi.org/10.1530/JOE-13-0616.
Park, J.H., Ku, H.J., Kim, J.K., Park, J.W., Lee, J.H., 2018. Amelioration of high fructose-induced cardiac hypertrophy by naringin. Sci. Rep. 8 (1), 9464. https://doi.org/10.1038/s41598-018-27788-1.
Pearce, E.L., Pearce, E.J., 2013. Metabolic pathways in immune cell activation and quiescence. Immunity 38 (4), 633–643. https://doi.org/10.1016/j.immuni.2013.04.005.
Pernagallo, S., Unciti-Broceta, A., Díaz-Mochón, J.J., Bradley, M., 2008. Deciphering cellular morphology and biocompatibility using polymer microarrays. Biomed. Mater. 3 (3), 034112. https://doi.org/10.1088/1748-6041/3/3/034112.
Prieto-Domínguez, N., Garcia-Mediavilla, M.V., Sanchez-Campos, S., Mauriz, J.L., Gonzalez-Gallego, J., 2018. Autophagy as a molecular target of flavonoids underlying their protective effects in human disease. Curr. Med. Chem. 25 (7), 814–838. https://doi.org/10.2174/0929867324666170918125155.
Rabinowitz, J.D., White, E., 2010. Autophagy and metabolism. Science 330 (6009), 1344–1348. https://doi.org/10.1126/science.1193497.
Ramkumar, A., Murthy, D., Raja, D.A., Singh, A., Krishnan, A., Khanna, S., Vats, A., Thukral, L., Sharma, P., Sivasubbu, S., Rani, R., Natarajan, V.T., Gokhale, R.S., 2017. Classical autophagy proteins LC3B and ATG4B facilitate melanosome movement on cytoskeletal tracks. Autophagy 13 (8), 1331–1347. https://doi.org/10.1080/15548627.2017.1327509.
Scholte, M., Timmers, L., Bernink, F.J., Denham, R.N., Beek, A.M., Kamp, O., Diamant, M., Horrevoets, A.J., Niessen, H.W., Chen, W.Y., Rossum, A.C., Royen, N.V., Doevendans, P.A., Appelman, Y., 2011. Effect of additional treatment with exenatide in patients with an acute myocardial infarction (EXAMI): study protocol for a randomized controlled trial. Trials 12 (1), 240. https://doi.org/10.1186/1745-6215-12-240.
Shi, R.Y., Weng, J.Q., Zhao, L., Li, X.M., Gao, T.M., Kong, J., 2012. Excessive autophagy contributes to neuron death in cerebral ischemia. CNS Neurosci. Ther. 18 (3), 250–260. https://doi.org/10.1111/j.1755-5949.2012.00295.x.
Soisungwan, S., Vesey, D.A., Gobe, G.C., 2017. Kidney cadmium toxicity, diabetes and high blood pressure: the perfect storm. Tohoku J. Exp. Med. 241 (1), 65–87. https://doi.org/10.1620/tjem.241.65.
Sutton, M.N., Yang, H., Huang, G.Y., Fu, C., Bast, R.C., 2018. Ras-related GTPases DIRAS1 and DIRAS2 induce autophagic cancer cell death and are required for autophagy in murine ovarian cancer cells. Autophagy 14 (1). https://doi.org/10.1080/15548627.2018.1427022. 01-47.
Tobias, H., Monika, P., Andreas, H., 2014. Snack food intake in ad libitum fed rats is triggered by the combination of fat and carbohydrates. Front. Psychol. 5, 250. https://doi.org/10.3389/fpsyg.2014.00250.
Torres, A., Gubbiotti, M.A., Iozzo, R.V., 2017. Decorin-inducible Peg3 evokes Beclin 1-mediated autophagy and thrombospondin 1-mediated angiostasis. J. Biol. Chem. 292 (12), 5055–5069. https://doi.org/10.1074/jbc.M116.753632.
Valente, G., Morani, F., Nicotra, G., Fusco, N., Peracchio, C., Titone, R., Alabiso, O., Arisio, R., Katsaros, D., Benedetto, C., Isidoro, C., 2014. Expression and clinical significance of the autophagy proteins Beclin-1 and LC3 in ovarian cancer. J. Biomed. Biotechnol. 2014 (8), 462658. https://doi.org/10.1155/2014/462658.
Vazhappilly, C.G., Ansari, S.A., Al-Jaleeli, R., Al-Azawi, A.M., Ramadan, W.S., Menon, V., Hodeify, R., Siddiqui, S.S., Merheb, M., Matar, R., Radhakrishnan, R., 2019. Role of flavonoids in thrombotic, cardiovascular, and inflammatory diseases. Inflammopharmacology 27 (5), 863–869. https://doi.org/10.1007/s10787-019-00612-6.
Wang, X.F., Luo, G.T., Zhang, K.D., Cao, J., Huang, C., Jiang, T., Liu, B., Su, L., Qiu, Z., 2018. Hypoxic tumor-derived exosomal miR-301a mediates M2 macrophage polarization via PTEN/PI3Kγ to promote pancreatic cancer metastasis. Canc. Res. 78 (16), 4586–4598. https://doi.org/10.1158/0008-5472.CAN-17-3841.
Xilouri, M., Brekk, O.R., Polissidis, A., Chrysanthou-Piterou, M., Kloukina, I., Stefanis, L., 2016. Impairment of chaperone-mediated autophagy induces dopaminergic neurodegeneration in rats. Autophagy 12 (11), 2230–2247 doi:10.80/15548627.2016.1214777.
Xue, J.F., Shi, Z.M., Zou, J., Li, X.L., 2017. Inhibition of PI3K/AKT/mTOR signaling pathway promotes autophagy of articular chondrocytes and attenuates inflammatory response in rats with osteoarthritis. Biomed. Pharmacother. 89, 1252–1261. https://doi.org/10.1016/j.biopha.2017.01.130.
Yang, Z., Zeng, B., Pan, Y., Huang, P., Wang, C., 2018. Autophagy participates in isoliquiritigenined/duced melanin degradation in human epidermal keratinocytes through PI3K/AKT/mTOR signaling. Biomed. Pharmacother. 97, 248–254. https://doi.org/10.1016/j.biopha.2017.10.070.
Yin, W.Y., Ye, Q., Huang, H.J., Xia, N.G., Chen, Y.Y., Zhang, Y., Qu, Q.M., 2016. Salidroside protects cortical neurons against glutamate-induced cytotoxicity by inhibiting autophagy. Mol. Cell. Biochem. 419 (1–2), 53–64. https://doi.org/10.1007/s11010-016-2749-3.
Zabala-Letona, A., Arruabarren-Aaristorena, A., Martín-Martín, N., Fernandez-Ruiz, S., Sutherland, J.D., Clasquin, M., Tomas-Cortazar, J., Jimenez, J., Torres, I., Quang, P., Ximenez-Embun, P., Bago, R., Ugalde-Olano, A., Loizaga-Iriarte, A., Lacasa-Viscasillas, I., Unda, M., Torrano, V., Cabrera, D., van Liempd, S.M., Cendon, Y., Castro, E., Murray, S., Revandkar, A., Alimonti, A., Zhang, Y., Barnett, A., Lein, G., Pirman, D., Cortazar, A.R., Arreal, L., Prudkin, L., Astobiza, I., Valcarcel-Jimenez, L., Zuñiga-García, P., Fernandez-Dominguez, I., Piva, M., Caro-Maldonado, A., Sánchez-Mosquera, P., Castillo-Martín, M., Serra, V., Beraza, N., Gentilella, A., Thomas, G., Azkargorta, M., Elortza, F., Farràs, R., Olmos, D., Efeyan, A., Anguita, J., Muñoz, J., Falcón-Pérez, J.M., Barrio, R., Macarulla, T., Mato, J.M., Martinez-Chantar, M.L., Cordon-Cardo, C., Aransay, A.M., Marks, K., Baselga, J., Tabernero, J., Nuciforo, P., Manning, B.D., Marjon, K., Carracedo, A., 2017. mTORC1-dependent AMD1 regulation sustains polyamine metabolism in prostate cancer. Nature 547 (7661), 109–113. https://doi.org/10.1038/nature22964.
Zeng, X., Bai, Y., Peng, W., Su, W., 2016. Identification of naringin metabolites in human urine and feces. Eur. J. Drug Metab. Pharmacokinet. 42 (4), 647–656. https://doi.org/10.1007/s13318-016-0380-z.
Zhang, Y., Zhan, R.X., Chen, J.Q., Gao, Y., Chen, L., Kong, Y., Zhong, X.J., Liu, M.Q., Chu, J.J., Yan, G.Q., Li, T., He, M., Huang, Q.R., 2015. Pharmacological activation of PPAR gamma ameliorates vascular endothelial insulin resistance via a non-canonical PPAR gamma-dependent nuclear factor-kappa B trans-repression pathway. Eur. J. Pharmacol. 754, 41–51. https://doi.org/10.1016/j.ejphar.2015.02.004.
Zhang, B., Chen, Y.P., Shen, Q., Liu, G.Y., Ye, J.X., Sun, G.B., Sun, X., 2016. Myricitrin attenuates high glucose-induced apoptosis through activating Akt-Nrf2 signaling in H9c2 cardiomyocytes. Molecules 21 (7), 880. https://doi.org/10.3390/molecules21070880.